Available online at www.sciencedirect.com
SCIENCE DIRECT®
Icarus 173 (2005) 3–15
ICARUS
www.elsevier.com/locate/icarus

Interpreting photometry of regolith-like surfaces with different topographies: shadowing and multiple scattering ☆

Yuriy G. Shkuratov [a,*], Dmitriy G. Stankevich [a], Dmitriy V. Petrov [a], Patrick C. Pinet [b], Aurélien M. Cord [b], Yves H. Daydou [b], Serge D. Chevrel [b]

[a] *Astronomical Institute of Kharkov National University, 35 Sumskaya St., Kharkov 61022, Ukraine*
[b] *Observatoire Midi-Pyrénées. 14 Av. E. Belin, 31400 Toulouse, France*

Received 28 June 2003; revised 29 November 2003

Available online 4 February 2004

Abstract

The effects of various types of topography on the shadow-hiding effect and multiple scattering in particulate surfaces are studied. Two bounding cases were examined: (1) the characteristic scale of the topography is much larger than the surface particle size, and (2) the characteristic scale of the topography is comparable to the surface particle size. A Monte Carlo ray-tracing method (i.e., geometric optics approximation) was used to simulate light scattering. The computer modeling shows that rocky topographies generated by randomly distributed stones over a flat surface reveal much steeper phase curves than surface with random topography generated from Gaussian statistics of heights and slopes. This is because rocks may have surface slopes greater than 90°. Consideration of rocky topography is important for interpreting rover observations. We show the roughness parameter in the Hapke model to be slightly underestimated for bright planetary surfaces, as the model neglects multiple scattering on large-scale topographies. The multiple scattering effect also explains the weak spectral dependences of the roughness parameter in Hapke's model found by some authors. Multiple scattering between different parts of a rough surface suppresses the effect of shadowing, thus the effects produced by increases in albedo on the photometric behavior of a surface can be compensated for with the proper decreases in surface roughness. This defines an effective (photometric) roughness for a surface. The interchangeability of albedo and roughness is shown to be possible with fairly high accuracy for large-scale random topography. For planetary surfaces that have a hierarchically arranged large-scale random topography, predictions made with the Hapke model can significantly differ from real values of roughness. Particulate media with surface borders complicated by Gaussian or clumpy random topographies with characteristic scale comparable to the particle size reveal different photometric behaviors in comparison with particulate surfaces that are flat or the scale of their topographies is much larger than the particle size.

Keywords: Photometry; Regoliths; Radiative transfer; Computer techniques

1. Introduction

Interpretations of spectroscopic, photometric, and polarimetric observations of planetary regoliths are currently based on theoretical modeling and computer and laboratory simulations of light scattering by particulate media. A widely accepted theoretical model describing such scattering has been developed by Bruce Hapke (1981, 1984, 1986, 1993, 2002) and has been used to analyze the surfaces properties of the Moon, Mercury, asteroids, and satellites. However, Hapke's model has simplifications and limitations that should be studied and understood. Attempts to improve the theory by making the basic formulas more rigorous are still impractical for application to planetary observations. For instance, the theory of multiple scattering by Mishchenko et al. (1999), which is suggested instead of Hapke's model, paradoxically ignores the shadow-hiding effect and the effect of coherent backscattering enhancement, though these effects are very significant for both dark and bright planetary regoliths. Computer and laboratory experiments are the most effective way to verify any photometric model and to investigate how it can be improved. Our computer simulations, providing an exact consideration of light scattering in particulate surfaces in geometric optics approximation, have demonstrated (Stankevich and Shkuratov, 2002) fairly

☆ This paper was presented at the Symposium "Solar System Remote Sensing," September 20–22, 2002, Pittsburgh, PA, USA.

* Corresponding author.
E-mail address: shkuratov@astron.kharkov.ua (Y.G. Shkuratov).

0019-1035/$ – see front matter
doi:10.1016/j.icarus.2003.12.017

good accordance of the Hapke model with benchmark data of computer experiments. This paper studies the roles of the shadow-hiding effect and multiple scattering for regolith-like surfaces with different boundary topographies in order to clear up how the Hapke model could be improved.

There are at least two motivations to study light scattering in particulate surfaces with complicated boundaries. One of them is the necessity for deeper analysis of physical mechanisms contributed to light scattering in planetary surfaces. The second one is of practical interest; it relates to interpretation of photometric observations with martian and lunar rovers, like Lunokhod-1, -2, the Mars Pathfinder and MER-A, -B vehicles. In situ photometric observations deal with surface resolution of about 0.1–1 cm. One cannot expect a priori that any photometric model applied satisfactorily to integral planetary observations or to large portions of a planetary surface with moderate resolutions (> 100 m per pixel) will give good results on roughness scales 0.1–1 cm (Cord et al., 2003c; Shkuratov, 2002; Stankevich et al., 2002). The martian and lunar surfaces have micro- and meso-topography that is complicated with stones and fairly steep undulations (clumps) of the particulate surface boundary. We consider the mentioned motivations in more detail.

1.1. Physical mechanisms

The important mechanisms for interpreting planetary photometric data are shadowing in particulate media (as well as on random surface topographies) and multiple scattering (incoherent and coherent). This study concentrates on shadowing and incoherent multiple scattering effects. The coherent backscatter enhancement effect has been studied in detail elsewhere (e.g., Hapke, 1990, 1993, 2002; Shkuratov et al., 1999, 2002).

Shadowing in particulate media is the important contributor to the photometric properties of the planetary regoliths at all phase angles even for highly reflective regolith surfaces (e.g., Hapke, 1981, 1986, 1993). Although, the shadow-hiding effect in regolith-like surfaces has been well studied, there are still unresolved and insufficiently studied issues (e.g., Shkuratov, 2002). For instance, the influence of shadowing on the different orders of multiple scattering has not been well investigated.

At large scales (> 100 m), planetary regolith surfaces have topographies that can be described by random single-valued functions (see Fig. 1, case 1). Such topographies influence brightness phase curves primarily at large phase angles. First approximation models accounting for the influence were presented by Smith (1967) and Hapke (1984, 1993) and used in many applications. Improvements of the analytical models are very difficult, as the rigorous description of shadowing even for random single-valued surfaces demands continual integrations (e.g., Shkuratov et al., 2000 and references therein).

The shadowing effect for surface and particulate structures that are hierarchically-arranged (Fig. 1, cases 2 and 7, respectively) have also been examined (Shkuratov, 1995; Shkuratov and Helfenstein, 2001; Shkuratov et al., 1994, 2003), since planetary surfaces have some attributes of physical fractals.

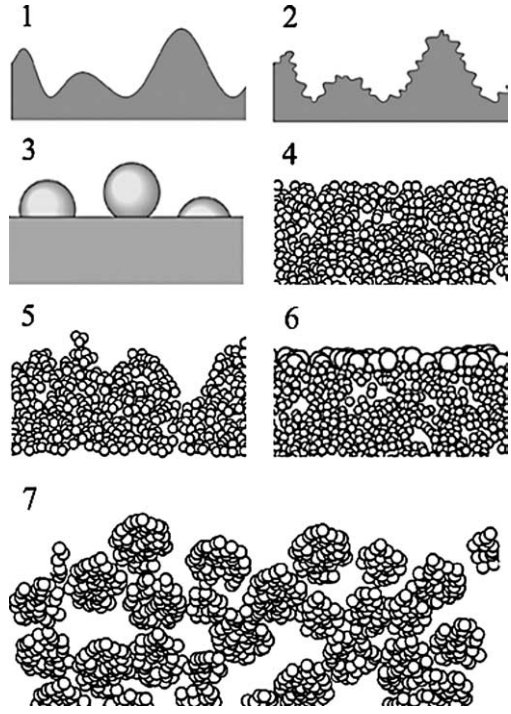

Fig. 1. Types of topographies: (1) simple random Gaussian topography, (2) hierarchically-arranged random Gaussian topography, (3) rocky topography, (4) particulate topography, (5) simple random Gaussian topography of particulate surface, (6) rocky topography for particulate surface, and (7) clumpy random topography of particulate surface.

The domain when the characteristic scale of surface topography is comparable with the size of surface particles (cf. cases 4 and 5 in Fig. 1) has been insufficiently studied both in terms of theoretical and experimental approaches (Helfenstein and Shepard, 1999; Pinet et al., 2001). For this size domain, details of the surface topography can be semi-transparent for direct rays from the light source producing additional problems with calculating the shadow-hiding effect.

If a regolith-like surface is weakly absorbing, incoherent multiple scattering can contribute considerably to photometric properties over the whole range of phase angles. The scattering may take place inside and between particles of a particulate surface, as well as between elements of the surface's topography. Multiple scattering in a particle, which is implied as a sequence of light reflections inside the particle, may be considered when the particle size is significantly larger than the wavelength. Geometric optics for such particles is applicable (e.g., Grynko and Shkuratov, 2003; Shkuratov and Grynko, 2004). We study here only interparticle incoherent multiple scattering.

The radiative transfer equation is usually used to calculate phase curves of a particulate media that account for interparticle multiple scattering (e.g., Hapke, 1981, 1993, 2002).

However, this equation does not take into consideration the correlation in the propagation of rays in the medium, which is responsible for the shadow-hiding effect (e.g., Shkuratov et al., 2000). The effect has been approximated in the radiative transfer theory for single scattered component (e.g., Hapke, 1981, 1993, 2002), however, the correlation producing the shadow-hiding effect also affects higher orders of scattering (Stankevich and Shkuratov, 2002).

Another important aspect of multiple scattering is the scattering between surface topography elements. The Hapke model does not consider this. The aspect is important for bright planetary surfaces. The multiple scattering between surface topography elements results in a decrease of the effective surface roughness (e.g., Shkuratov et al., 1994; Shepard and Campbell, 1998; Shepard et al., 2001).

The most complicated case is when the characteristic scale of the surface topography is close to the particle size. This case is rather typical as any real particulate medium has a transition upper layer that is formed due to vertical fluctuations of particles near the average level (see Fig. 1, case 4). The transition layer can strongly influence calculated phase curves of multiple and especially single scattering (Stankevich and Shkuratov, 2000).

All these issues are difficult to be solved analytically, however, they can be well studied via computer simulations.

1.2. Resolution effects

Substantial increase in the spatial resolution of planetary optical experiments (e.g., multispectral measurements for the Mars Pathfinder, Mars Express, and MER-A, -B missions) requires the analysis of the effects of observation/illumination conditions on the bidirectional reflectance of surfaces composed of rocks and rock-and-soil mixtures. To model observations of different surfaces including rocky surfaces, a new spectral imaging facility has been designed at the Observatory Midi-Pyrenees (Pinet et al., 2001). First results concerning the influence of the meso-scale textural topography on the roughness parameter have been obtained (Cord et al., 2002, 2003a, 2003b, 2003c). In particular, attempts to interpret laboratory measurements carried out with the facility have been made using the Hapke model. Fitting of the model parameters to the laboratory measurements produces, in some cases, nonunique solution resulting in ambiguous physical interpretation; the same was found earlier for planetary data (e.g., Helfenstein et al., 1988). Indeed, the Hapke model implicitly assumes the scale of surface topography to be much larger than the size of regolith particles composing a particulate medium. Besides, this model describes topography with a single-valued random function. However, in laboratory and in situ planetary measurements one may deal with other types of surface topography. For instance, topographies formed with rocks and/or particle clumps, generally, have characteristic scales comparable with the size of regolith particles (see Fig. 1, cases 3, 6, 7). Initial results from the facility (Cord et al., 2003c) show that for a flat powdered surface with grain size < 75 μm the surface roughness θ (the angle of the surface RMS slope in the Hapke model) ranges between 6° and 15°, thus demonstrating that the roughness cannot be neglected.

Our study demonstrates the importance of surface topography in interpreting photometry of regolith-like surfaces. We use here new computer modeling results based on geometric optics. Single and incoherent multiple scattering by the following surfaces is examined:

(1) random single-valued topography with the characteristic scale much larger than the particle size (Fig. 1, case 1);
(2) random hierarchically-arranged topography with the minimal characteristic scale much larger than the particle size (Fig. 1, case 2);
(3) random rocky topography with the characteristic scale much larger than particle size (Fig. 1, case 3);
(4) statistically flat particulate surface (Fig. 1, case 4);
(5) random single-valued topography with the characteristic scale somewhat larger than the particle size (Fig. 1, case 5);
(6) random rocky topography with the characteristic scale somewhat larger than the particle size (Fig. 1, case 6);
(7) random clumpy topography with the characteristic scales somewhat larger than the particle size (Fig. 1, case 7).

When the characteristic scale of the topography is much larger than the particle size, the surface can be regarded as continuous with a known indicatrix of surface elements. This study uses a Lambertian indicatrix, though any indicatrix could be incorporated. If the characteristic scale of the topography is comparable with the particle size, the enveloping surface cannot be considered as continuous. This case is fairly realistic, e.g., the hierarchical particulate topography (see Fig. 1, case 7) is a model of media composed of aggregated particles like the lunar regolith that contains much agglutinates. The rocky topography is simulated using spheres randomly embedded in a surface. This case can be attributed to continuous surfaces (Fig. 1, case 3), when the spheres and distances between them are much larger than the particle size, and to particulate surfaces (Fig. 1, case 6), when "rocks" and distances between them are somewhat larger than particle size. Another interesting example of complex particulate surfaces is media consisting of particles with different albedo forming optically contrasting domains of different scales. However, this example, being rather diverse, requires a special consideration (e.g., Stankevich and Shkuratov, 2004) and is not examined in this study.

2. Computer models

We use two ray-tracing models to study single and multiple light scattering of light by both continuous and particulate surfaces with complicated boundaries. Particles are con-

sidered to be opaque with the Lambertian indicatrix of their surface elements (continuous surfaces are also described by the Lambertian indicatrix). It should be noted that the integral scattering indicatrix of such a particle is elongated in the backward direction. This elongation decreases the role of multiple scattering in the media. Indeed, even at conservative (nonabsorbing) scattering, the contribution of high orders of interparticle scattering to the total medium reflectivity equals zero, if the particle indicatrix is the δ-function directed rigorously to/from the light source. Multiple scattering is computed using single scattering albedo ω of the particle surface element.

2.1. Continuous surfaces

We investigate random single-valued continuous surfaces with Gaussian statistics of heights and slopes. In addition, we study hierarchically-arranged continuous surfaces, for which each generation level is presented by a simple Gaussian random surface. As a prototype we incorporate the computer model exploited for calculations of the shadow-hiding effect (Shkuratov and Stankevich, 1992; Stankevich and Shkuratov, 1992). Portions of the surfaces (finite realizations), which are large enough, are used for the following ray-tracing procedure. An initial ray is traced from a random point of the surface in the direction of a light source. This ray can either leave the surface without interruption (and hence the point is illuminated) or intersects the surface (and hence the point is shaded). Next, a new ray is traced from the point in the direction of an observer. If this ray does not intersect the surface, the point is visible. If the point is both visible and illuminated, it contributes to the intensity of the single scattered light. To calculate the second scattering order, we trace a ray from a visible point (point 1) in a random direction. If the ray intersects the surface at an illuminated point (point 2), this contributes to the intensity of the double scattered light. To calculate higher scattering orders, we repeat these steps taking into account that if a ray does not intersect the surface or intersect it at a nonilluminated point, its contribution equals zero. The procedure is repeated many times from the very beginning for different surface points to reach desired accuracy of the ray-tracing process at calculation of all needed scattering orders.

2.2. Particulate surfaces

We have used and described many times a ray-tracing model for particulate surfaces with macroscopically flat boundaries to calculate the shadow-hiding effect and multiple scattering (e.g, Stankevich et al., 1999, 2000, 2003; Stankevich and Shkuratov, 2000, 2002; Muinonen et al., 2001). To take roughness of a particulate surface into account we produce an update computer model that is able to deal with larger number of particles.

We simulate with the models what happens in nature or laboratory studies. A large random system of opaque diffusely scattering particles is generated in a computer memory and is "illuminated" by rays that are traced in the system from a light source to an observer. Unlike the previous model, the updated model is able to effectively simulate multiple scattering in semiinfinite particulate media with arbitrary surface topographies having the characteristic scale a little larger than the size of the medium's particles. For the sake of simplicity the particles are assumed to be spherical and uniform. The updated model has two separate stages:

(1) generation of a random system of particles with a certain volume density ρ, and
(2) Monte Carlo ray tracing.

We use a system of particles randomly distributed in a cube. The upper border of this cube can be complicated by a topography. The lateral and bottom sides are considered to be cyclically closed, i.e., if a ray leaves the cubic volume, e.g., through a lateral side, it comes into the same volume from the opposite side. This is a way to simulate a semiinfinite medium using a finite volume.

The quality of our previous model (Stankevich et al., 1999, 2000, 2003; Stankevich and Shkuratov, 2000, 2002) is limited by statistics. There are two main sources of statistical errors: the limited number of particles in the model volume (it was $N = 8000$) and the limited number of traced rays (normally $R = 10000$). Increases of these numbers were restricted as computations become too long. The main problem is that each ray is inspected for intersection with each model particle, giving the total number of such inspections $RN = 8 \times 10^7$ for each phase angle. We improved the model by implementing some internal arranging of the model volume, subdividing the cube with a big number n^3 of small subcubes. Then a ray going through the model volume crosses only a small number of the subcubes ($\sim n$). Hence we need to examine the ray intersection with only the particles inside the current subcube and some adjacent ones. This gives the total number of the inspections $\ll RN$. Using this we have elaborated an improved algorithm allowing us at $n = 256$ to deal with $R = 10^6$ and the maximal $N = 16 \times 10^6$. Typically we use $N = 1.5 \times 10^6$, i.e., numbers of rays and particles are approximately equal to balance the two sources of statistical errors. As the radius of the largest particle cannot exceed the edge of small cube, the model does not incorporate particles with substantially different sizes.

3. Results and discussion

Although our model allows for calculations at arbitrary illumination/observation geometries, this study focuses on two of them:

(1) a mirror geometry ($i = \varepsilon = \alpha/2$, $\varphi = \pi$, where i and ε are the angles of incidence and emergence, respectively,

φ is the azimuthal angle between the planes of incidence and emergence, and α is the phase angle), and

(2) an azimuthal geometry ($i = \varepsilon = 85°$, $\varphi \approx \alpha$).

Below we present the results for single and multiple scattering by continuous and particulate surfaces at these two diverse geometries. To characterize a simple random surface with Gaussian statistics we use the parameter θ that corresponds to the surface RMS slope.

3.1. Scattering by continuous random surfaces

First of all, we consider single scattering by facets of a continuous Gaussian topography with $\theta = 45°$ (the RMS slope equals 1) and for rocky topography modeled with spherical "stones" randomly embedded in a substrate with a flat surface boundary (cf. cases 1 and 3 in Fig. 1). The volume density of the stone layer is taken 0.3. This density provides almost the same number of details of structure in the model frame as in case of the Gaussian topography. Shown in Fig. 2 are phase curves of the probability that a ray going from an illuminated point of the surface to an observer is not interrupted. Gaussian (G) and rocky (R) topographies at both the mirror (M) and azimuthal (A) geometries are presented in Fig. 2. As one can see at the mirror geometry the rocky topography demonstrates much steeper phase curve at small phase angles than in case of the Gaussian topography. This is quite reasonable as rocky topographies may have surface slope angles greater than $\pi/2$, producing shadows at small phase angles for any illumination/observation geometry. In contrast, the Gaussian surface produces shadows at the mirror geometry only when the values of $\alpha/2$ are greater than $\pi/2 - \theta$. At the azimuthal geometry the shadow-hiding probability for these different types of topography reveals a similar phase angle behavior. This demonstrates that the type of meso-scale topography exhibited by a surface is an important factor for calculating the shadow-hiding effect for planetary surfaces, especially in the context of coming rover explorations of Mars.

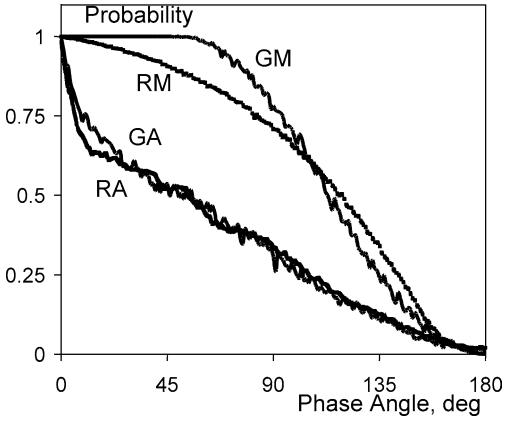

Fig. 2. Phase curves of the probability for simple random Gaussian (G) and rocky (R) topographies at the mirror (M) geometry and azimuthal (A) geometry.

Contributions from the different scattering orders to the total light flux from a randomly rough surface with Gaussian statistics decrease rapidly with increasing scattering order, even for rough surfaces at $\omega = 1$. Figures 3 and 4 illustrates this, showing phase curves for the mirror and azimuthal geometries, respectively, at surface slopes of $\theta = 20°$ and 40°. As can be predicted the contribution from the higher orders of scattering increases with increasing phase angle. Thus, for the azimuthal geometry at $\alpha > 145°$ ($\theta = 40°$) the total scattered flux is fully controlled by the second order of scattering. Rougher surfaces are characterized by larger contribution from the high scattering orders, as should be.

Multiple scattering of light between different parts of a rough surface suppresses the effect of shadowing. Hence the phase curve of a rough surface with high albedo has a lower slope than that of a dark surface with the same rough-

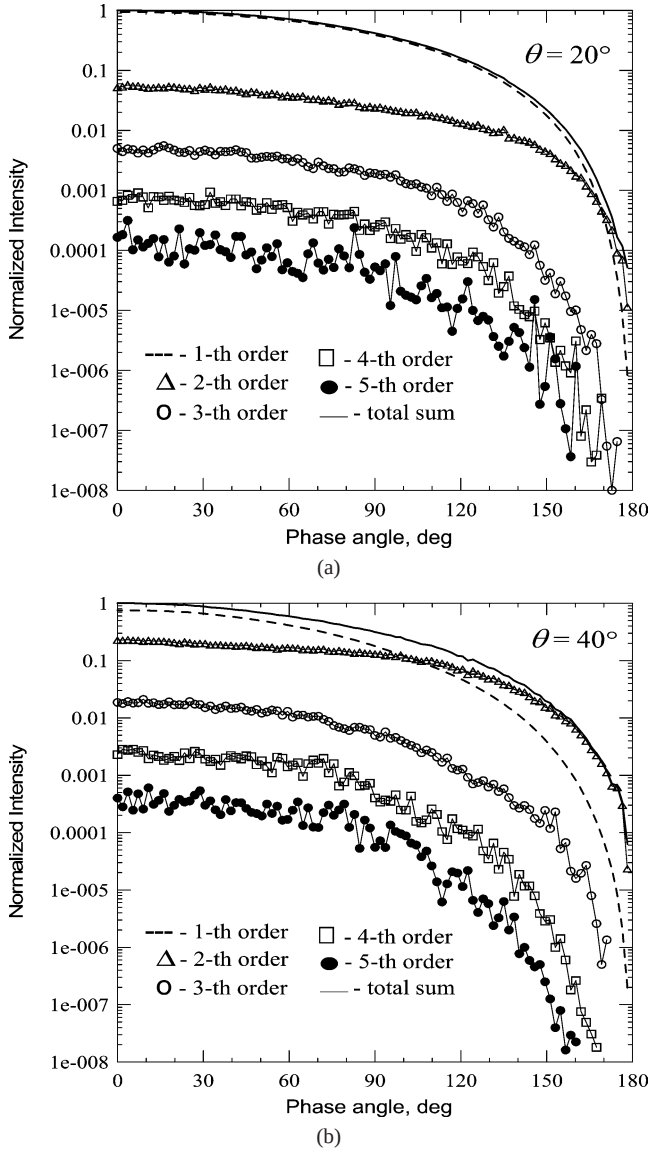

Fig. 3. Phase curves for separate orders and total sum at $\theta = 20°$ (a) and 40° (b) for the mirror geometry ($\omega = 1$).

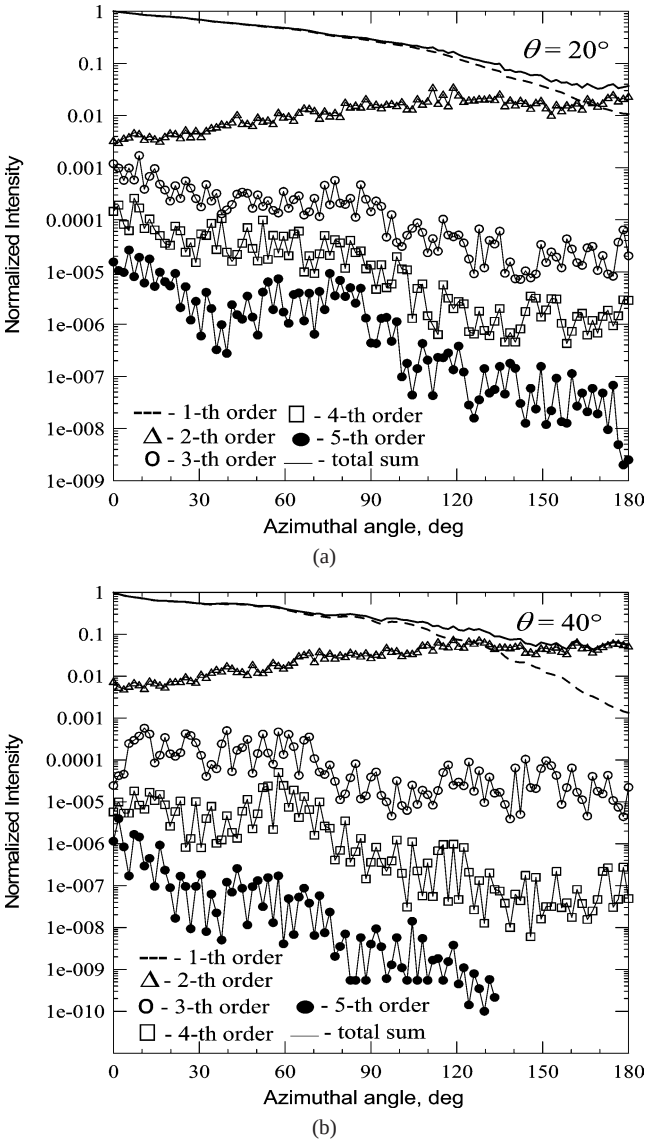

Fig. 4. Phase curves for separate orders and total sum at $\theta = 20°$ (a) and 40° (b) for the azimuthal geometry ($\omega = 1$).

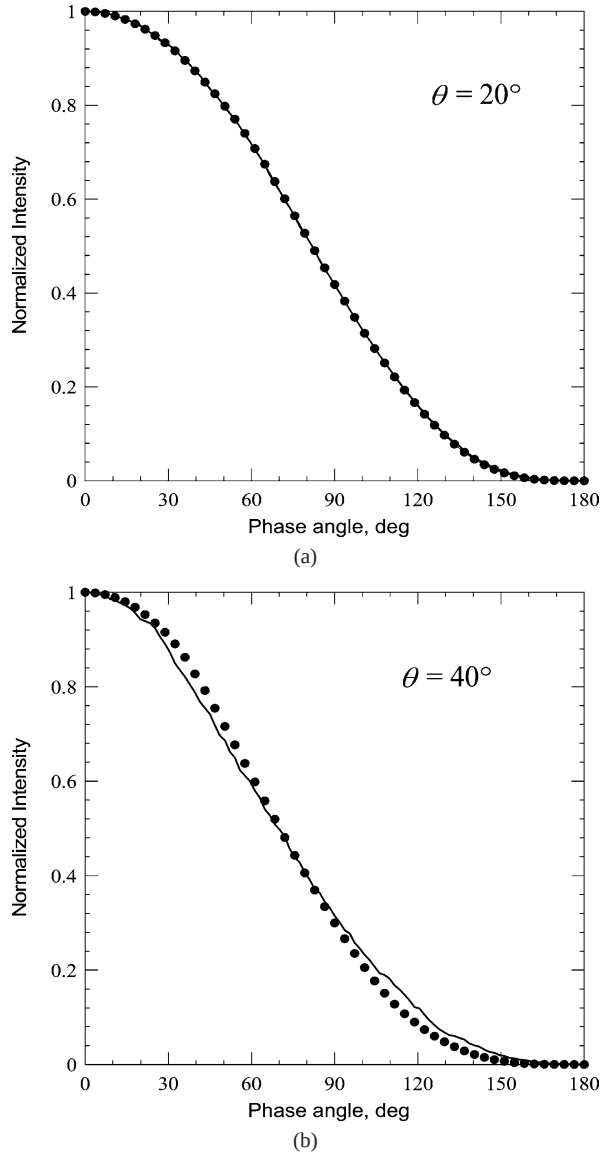

Fig. 5. Examples of phase curves for random Gaussian surfaces with $\theta = 20°$ (a) and 40° (b) at the mirror geometry (solid lines). The surfaces are absolutely white with the Lambertian indicatrix. Points correspond to the "equivalent" surfaces with $\theta_{\text{eff}} = 19.3°$ and 33.4°, respectively.

ness. Therefore, we can expect that the albedo increase may at least approximately be compensated for with an appropriate decrease in surface roughness. This defines an effective photometric roughness θ_{eff} that is dependent on albedo (e.g., Shkuratov et al., 1994; Shepard and Campbell, 1998; Shepard et al., 2001). Introducing the parameter θ_{eff} allows one to take the multiple scattering into account using the single scattering consideration. We examine this possibility below for continuous random surfaces with Gaussian statistics including the case of fractal-like topography.

Figure 5 presents phase curves (solid lines) for continuous random Gaussian surfaces with $\omega = 1$ and different RMS slopes ($\theta = 20°$ and 40°) in the mirror geometry. The first five scattering orders were taken into account (cf. Fig. 3). The single scattering order (points) appears to provide good fits by small decreases of θ. The least-squares method is used for the fitting. The differences between θ and θ_{eff} are fairly small: instead of 20° and 40° we obtain 19.3° and 33.4°, respectively. The quality of the fitting becomes worse with growth of roughness, however, even at $\theta = 40°$ the curves can still be very close to each other. One can observe the same for the azimuthal geometry (see Fig. 6), however, the differences between θ and θ_{eff} in this case distinct from those for the mirror geometry: instead of 20° and 40° we obtain 18.7° and 36.7°, respectively. Thus we may conclude that for rough surfaces with rather small θ, the effects of albedo and roughness on phase angle curves are approximately interchangeable. We have calculated dependences of θ_{eff} on θ for random Gaussian surfaces with different albedo ω at the mirror and azimuthal geometries (see Figs. 7 and 8). We note that for the mirror geometry the

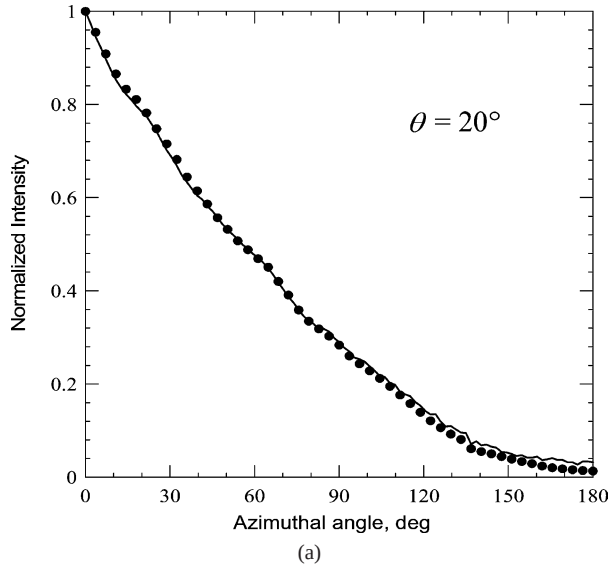

Fig. 6. Examples of phase curves for random Gaussian surfaces with $\theta = 20°$ (a) and 40° (b) at the azimuthal geometry (solid line). The surface is absolutely white with the Lambertian indicatrix. Points corresponds to the "equivalent" surface with $\theta_{\text{eff}} = 18.7°$ and 36.7°, respectively.

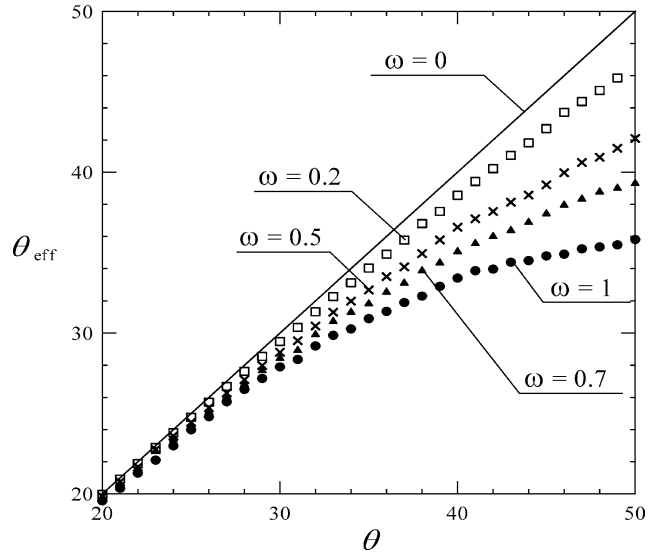

Fig. 7. Dependences of θ_{eff} on θ for random Gaussian surfaces with different albedo ω at the mirror geometry. The scales are given in degrees.

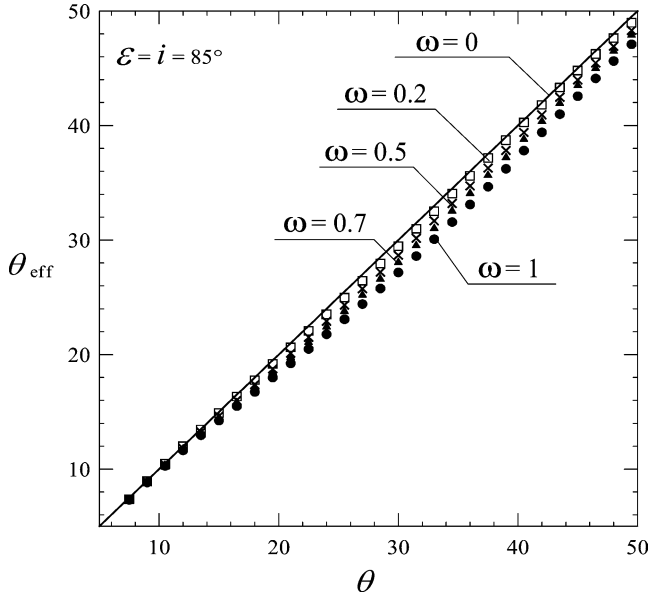

Fig. 8. Dependences of θ_{eff} on θ for random Gaussian surfaces with different albedo ω at the azimuthal geometry. The scales are given in degrees.

difference between θ and θ_{eff} is more than for the azimuthal geometry. The reason is that at the azimuthal geometry the contributions of high scattering orders are less than for the mirror geometry.

An analogous consideration can be carried out for hierarchical (fractal-like) topographies. We study here a topography with two hierarchical levels (each is a random Gaussian relief), when the large-scale topography is regarded as a reference surface for the small-scale topography (see Fig. 1, case 2). Figure 9 shows phase curves (solid lines) for fractal-like surfaces of 2-levels, each being a random Gaussian surface with $\theta = 20°$ and 40°, respectively. The calculations were made for the mirror geometry at $\omega = 1$. Points correspond to the "equivalent" surfaces that are a simple (1-level) random Gaussian topography with $\theta_{\text{eff}} = 25.5°$ and 46°, respectively. The effective characteristic angle is larger than θ, as we use the 1-level surface to simulate the 2-levels one. Presented in Fig. 10 is the same for the azimuthal geometry. It is amazing that for both these geometries simulating curves (points) provide fairly good fits to "actual" dependences (solid line). Like the simple topography, the 2-levels surface reveals difference in multiple scattering contributions for the mirror and azimuthal geometries.

As has been made above, we calculated θ_{eff} as a function of θ for 2-levels surfaces with different albedo ω at the mirror and azimuthal geometries (see Figs. 11 and 12). In this case we note again that for mirror geometry the difference

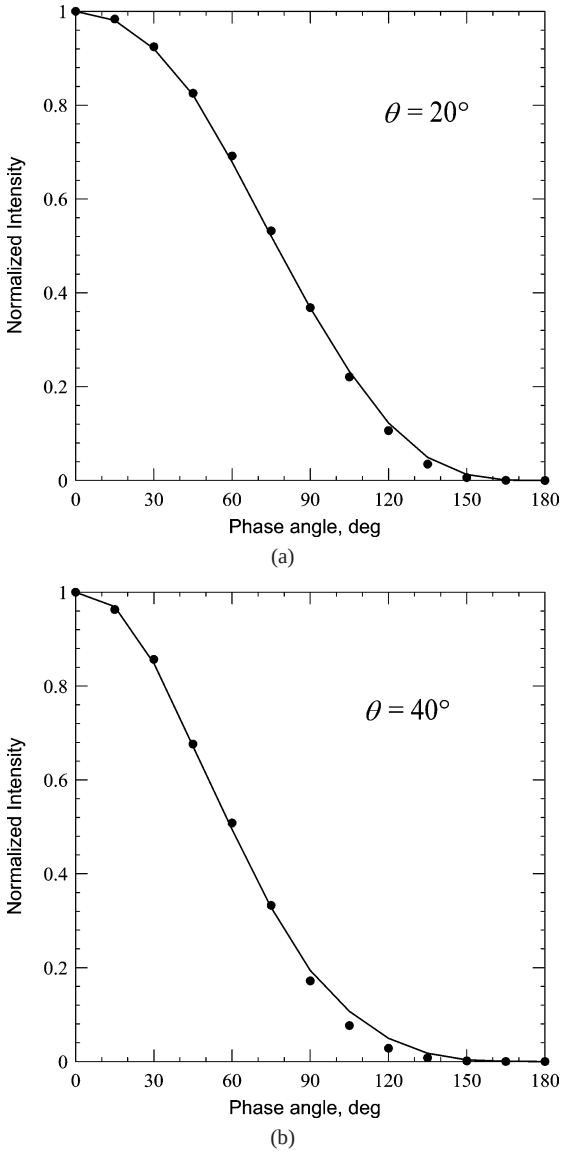

Fig. 9. Phase curves (solid lines) for hierarchical surfaces of 2-levels, each of which is a random Gaussian surface with $\theta = 20°$ (a) and 40° (b). The surfaces are absolutely white with the Lambertian indicatrix. Calculations were made for the mirror geometry. Points correspond to the "equivalent" surfaces that are simple random Gaussian topography with $\theta_{\text{eff}} = 25.5°$ and 46°, respectively.

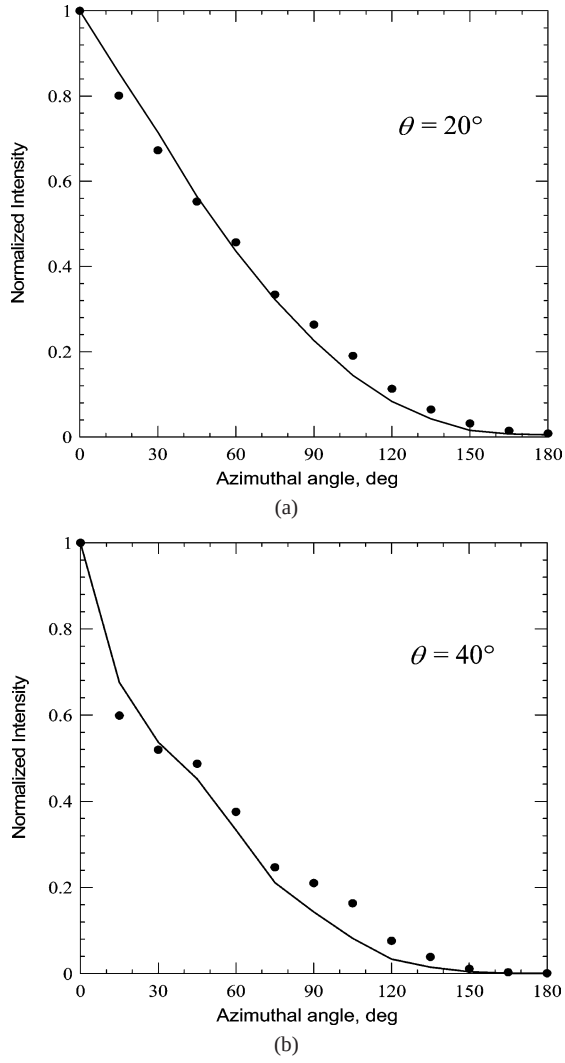

Fig. 10. Phase curves (solid lines) for hierarchical surfaces of 2-levels, each is a random Gaussian surface with $\theta = 20°$ (a) and 40° (b). The surfaces are absolutely white with the Lambertian indicatrix. Calculations were made for the azimuthal geometry. Points correspond to the "equivalent" surfaces that are simple random Gaussian topography with $\theta_{\text{eff}} = 22°$ and 45°, respectively.

between θ and θ_{eff} is more prominent, than that for the azimuthal geometry.

Thus we may summarize that accounting for multiple scattering on large-scale topographies with the characteristic angle $> 30°$ and albedo $> 20\%$ is important. As the Hapke model does not take multiple scattering into consideration, determinations of the roughness parameter with this model will be slightly underestimated. For example, if using a fit with the Hapke model one finds that θ of a rough surface with albedo 30% is 40°, this actually means that the parameter θ equals approximately 42° (see Figs. 7 and 8). Besides, in many fits with the Hapke model, workers have often found that the roughness parameter θ reveals an albedo dependence, recently reinvestigated in terms of spectral dependence (e.g., Cord et al., 2003a, 2003c). From the present results, we can offer an explanation for this puzzling feature with the contribution of multiple scattering. If a surface under study has a large-scale topography with the two-or-more-levels structure, predictions with the Hapke model can noticeably differ from real values. Besides, it should be emphasized that the influence of albedo on estimates of roughness increases when surface elements scatter light at large phase angles more effectively, than in case of the Lambertian indicatrix.

3.2. Scattering by particulate surfaces with rough boundary

We have also investigated the more complicated case where particulate surfaces have surface topographies with a

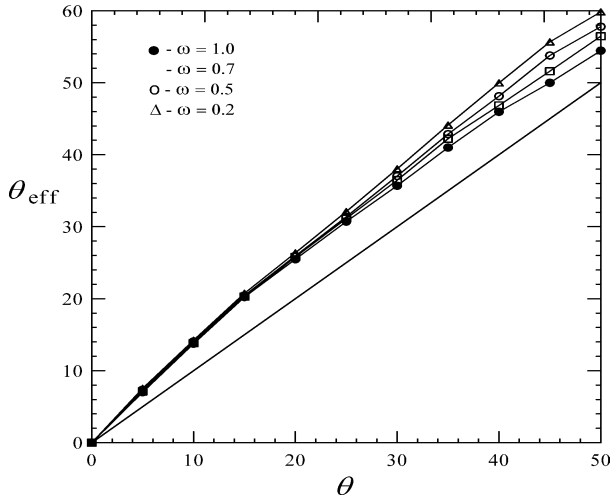

Fig. 11. Dependences of $\theta_{\rm eff}$ on θ for hierarchically-arranged surfaces formed with 2-levels which are random Gaussian surfaces with different albedo ω at the mirror geometry. The scales are given in degrees.

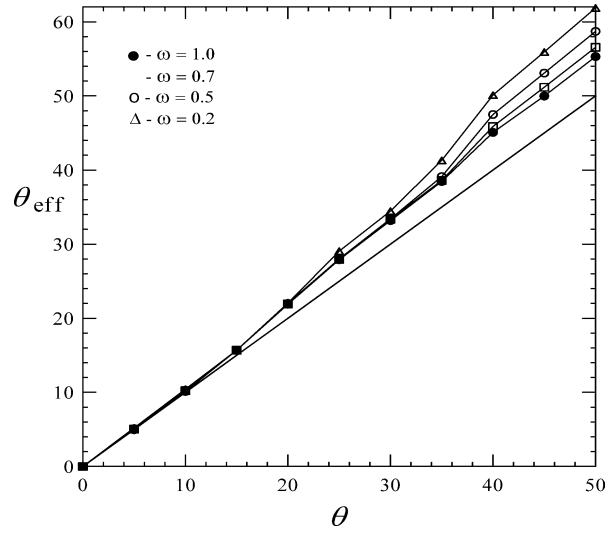

Fig. 12. Dependences of $\theta_{\rm eff}$ on θ for hierarchically-arranged surfaces formed with 2-levels that are random Gaussian surfaces with different albedo ω at the azimuthal geometry. The scales are given in degrees.

characteristic scale larger than the particle size. We compare four surface topographies:

(a) a statistically flat particulate surface (Fig. 1, case 4);
(b) a particulate surface undulated by random topography with a Gaussian distribution of heights and Gaussian correlation function (Fig. 1, case 5);
(c) a surface complicated with a layer of "rocks" randomly distributed (with random embedding) over a fine-grained particulate medium (Fig. 1, case 6); and
(d) a topography formed with clumps of particles (Fig. 1, case 7).

It should be noted that our computer model takes automatically into account all mutual correlations of all trajectories of

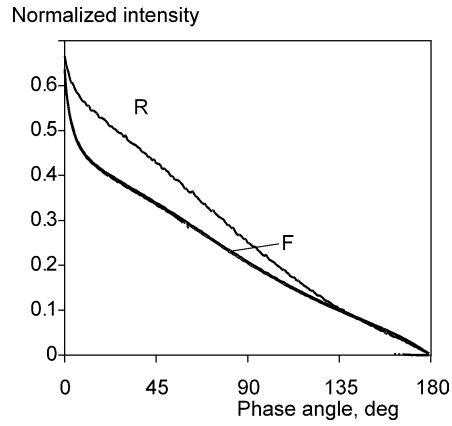

Fig. 13. Phase curves of reflectance for rocky (R) and flat-particulate (F) topographies at the mirror geometry.

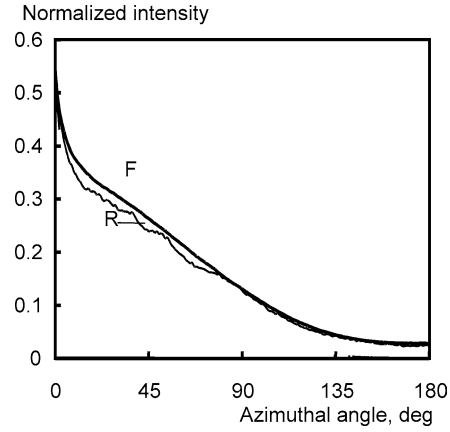

Fig. 14. Phase curves of reflectance for rocky (R) and flat particulate (F) topographies at the azimuthal geometry.

rays in particulate surfaces providing for the shadow-hiding effect for all scattering orders.

Phase curves for semiinfinite particulate media (with the volume density $\rho_{\rm m} = 0.1$), whose surfaces are statistically flat or complicated by rocks distributed with the volume density $\rho_{\rm r} = 0.3$, are presented in Figs. 13 and 14 for the mirror and azimuthal geometries, respectively. Multiple scattering is computed using five scattering orders. As a characteristic of the rocky relief, we use the radius of opaque "stones" $R = 10r$, where r is the radius of medium particles. This is a representative morphometric distribution observed in some experimental simulations (e.g., Cord et al., 2003c). We consider also that the thickness of the rocky layer equals $2R$ (see Fig. 1, case 6). Multiple scattering between rocks, rocks and medium particles, and within the particulate medium is taken into account. The brightness surges seen in Fig. 13 are due to the shadow-hiding effect. The surge is more prominent for the flat particulate medium (F). Opaque rocks superimposed on a flat particulate topography decrease the shadow-hiding surge as their surface is characterized by the Lambertian indicatrix that has not the opposition surge. For the azimuthal geometry both curves are very close to each other, since in

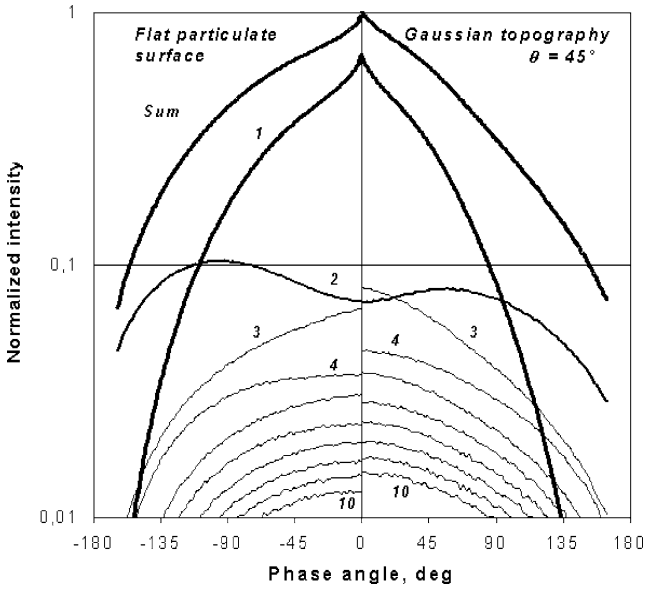

Fig. 15. Normalized phase curves of different scattering orders and sum for a random Gaussian particulate surface (right panel) in comparison with a flat particulate surface (left panel) at the mirror geometry.

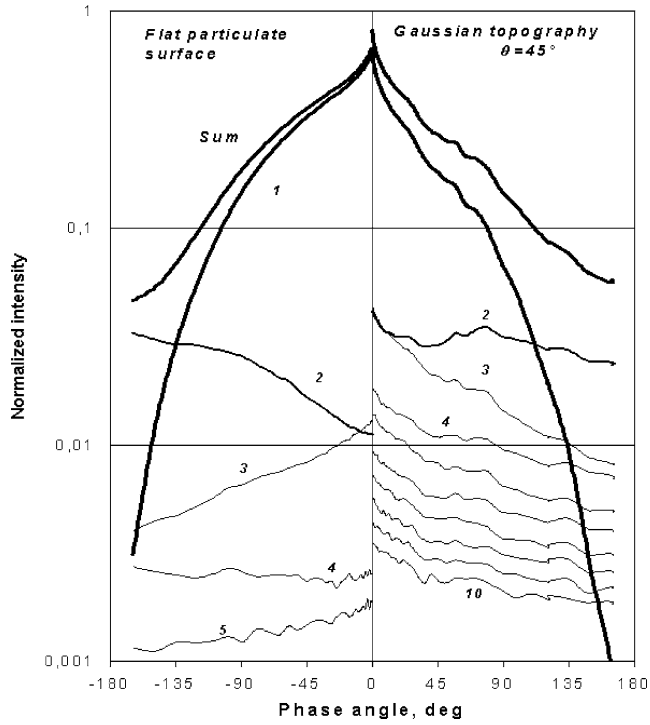

Fig. 16. Normalized phase curves of different scattering orders and sum for a random Gaussian particulate surface (right panel) in comparison with a flat particulate surface (left panel) at the azimuthal geometry.

this geometry a rocky topography can contribute to an opposition surge.

We also study the effect caused by surface topographies whose particulate details with the characteristic size L are small enough to be semitransparent. Random topographies with the Gaussian statistics of heights and slopes (Fig. 1, case 5) and the so-called clumpy topographies formed by aggregates of particles (Fig. 1, case 7) are investigated. We examine phase curves from different scattering orders with $\omega = 1$. Figure 15 presents data for 10 orders of scattering and their sum calculated for the mirror geometry. The right panel shows data for the random Gaussian particulate topography with $L = 10r$ and $\theta = 45°$ at $\rho = 0.3$. The conditions $L = 10r$ and $\theta = 45°$ imply that details of the topography are semitransparent for direct rays from the light source. For comparison, the left panel shows the equivalent case for a flat particulate surface. Predictably, curve (1) describing the single scattering is steeper for the surface with the Gaussian topography due to additional shadowing. In both these compared cases the double scattering shows maximum at moderate phase angles. For the flat surface this maximum is higher and placed at larger phase angles than in the case of the particulate surface with the Gaussian topography. At phase angles near 110°–120° intensities of the first and second scattering orders are equivalent for both particulate surfaces. This relationship between the first and second scattering orders is also seen for continuous surfaces at approximately the same phase angles (cf. Figs. 3b and 15). Figure 15 also shows that the role of the higher orders of scattering is more significant for rough surfaces. Moreover, at phase angles smaller than 30° the curve corresponding to the third scattering order lies higher than that of the second scattering order and has a steep slope.

A similar comparison for these two types of particulate surfaces was carried out in the azimuthal geometry (see Fig. 16). The data shown in the right panel are noisy because of poor ray statistics in the azimuthal geometry (angles of illumination and observation are 85°). As was above, in the mirror geometry case, the shadow-hiding effect is stronger for the rough surface. In the azimuthal geometry the difference between the values of the high scattering orders for flat versus rough particulate surfaces is much more prominent than in the previous mirror geometry. All orders are steeper for rough particulate surfaces because of the shadow-hiding effect on large-scale topography elements.

We studied the interchangeability of albedo and roughness for particulate surfaces like it has been examined above for continuous surfaces. It turns out that the interchangeability is not so well defined in this case. We cannot achieve satisfactory fits varying albedo and roughness. A good fit was found for the range of phase angles 10°–30° only. Figure 17 shows the phase ratio (10°/30°) as a function of the roughness parameter θ for the mirror and azimuthal geometries at two values of ω. It is interesting to note the interchangeability of albedo and surface roughness effects for the phase ratio to be possible in the azimuthal geometry only. This indicates that the phase ratio does not contain enough information for retrieving surface characteristics.

We also investigated clumpy topographies that are actually hierarchically arranged media (see Fig. 1, case 7). A medium composed of clumps with the volume density $\rho_{cl} = 0.3$ was generated and each clump is a piece of a

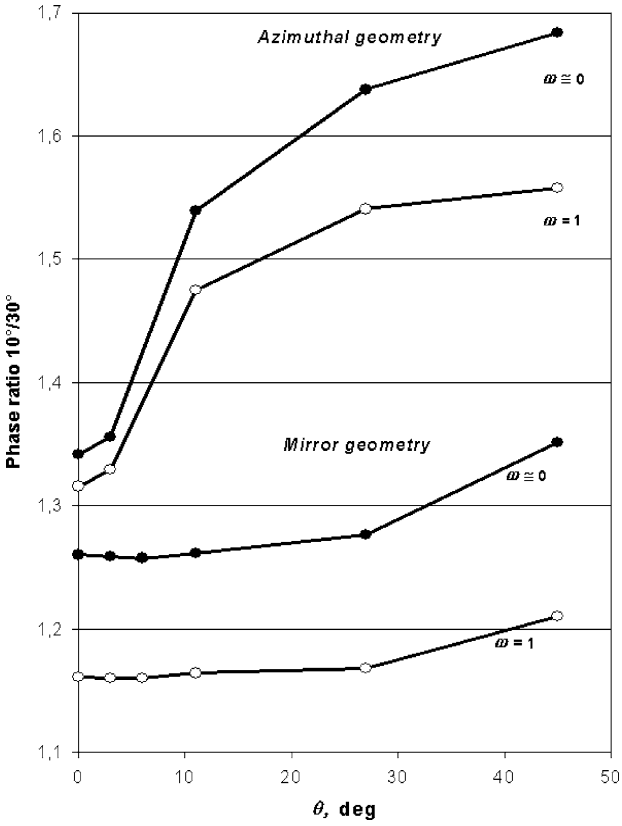

Fig. 17. The phase ratio $I(10^\circ)/I(30^\circ)$ as a function of θ for a random Gaussian particulate surfaces with different albedo ω at the mirror geometry.

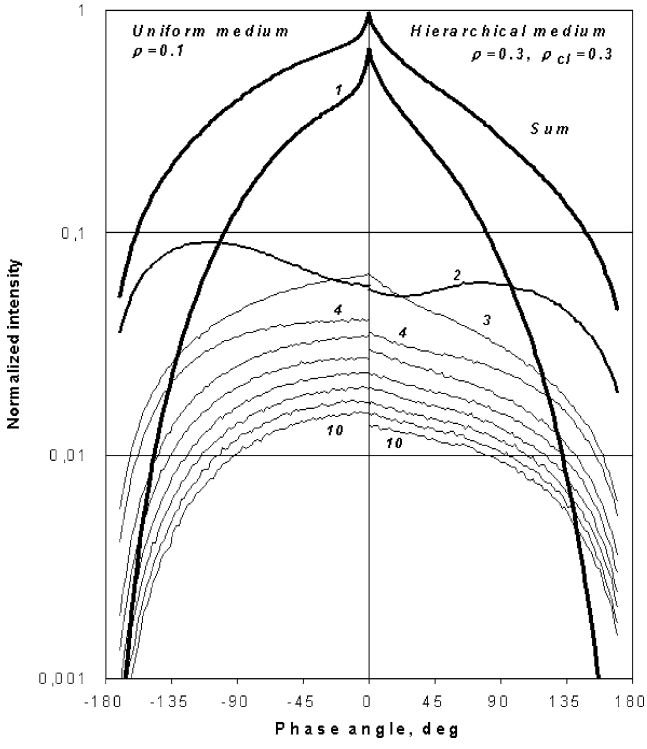

Fig. 18. Normalized phase curves of different scattering orders and sum for a clumpy particulate surface (right panel) in comparison with an equivalent flat particulate surface (left panel) at the mirror geometry.

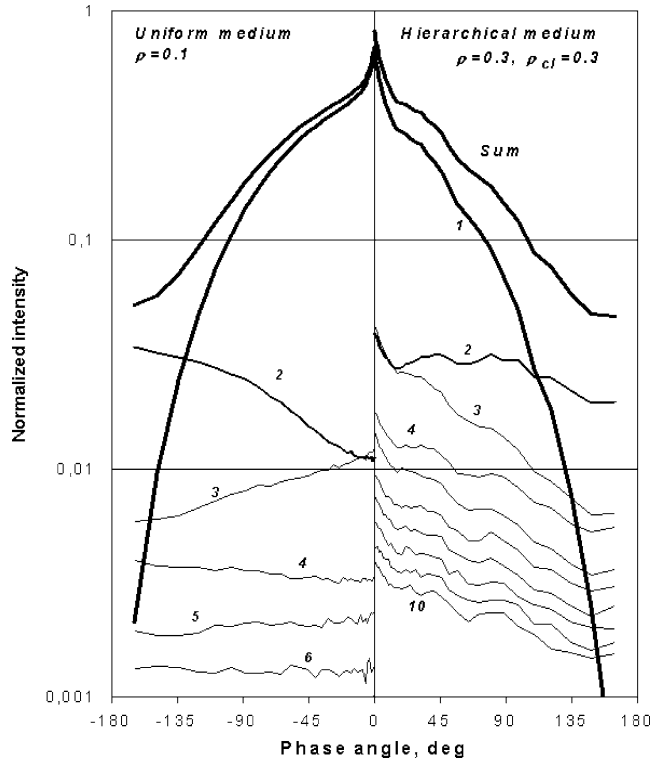

Fig. 19. Normalized phase curves of different scattering orders and sum for a clumpy particulate surface (right panel) in comparison with an equivalent flat particulate surface (left panel) at the mirror geometry.

medium with $\rho = 0.3$. Thus, the total volume density of the medium is $\rho = 0.09$. Figure 18 represents phase curves for different scattering orders and their sum for the hierarchical medium (right side) and for the equivalent medium without the clumpy structure (uniform medium) with $\rho = 0.1$ in the mirror geometry. As one can see the hierarchical medium exhibits more prominent shadow-hiding effect and weaker multiple scattering in comparison to uniform media. The same comparison has been carried out for the azimuthal geometry (see Fig. 19). The behavior of all the studied dependences of the clumpy topography is similar to those of the Gaussian topography of particulate surfaces.

4. Conclusion

Results from including surface topography in the modeling the border effects at calculations of the shadowing effect and multiple scattering in particulate media improves the interpretation of photometric observations of regolith-like surfaces. This investigation demonstrates the following:

(1) The shadow-hiding effect originating from both the particulate structure and border topography is significant even for the conservative case where the single scattering albedo is close to 1. Hence, any theories ignoring this fundamental effect (e.g., Mishchenko et al., 1999) should be used with great caution.

(2) The rocky surface topographies produce much steeper phase curves than those with a Gaussian surface topography. This is because rocks may create surface slope angles greater than 90°. The effect is important in the theoretical interpretation of photometric data obtained in situ for the martian and lunar surfaces.
(3) The quantitative interchangeability between albedo and surface roughness with large-scale topography is found. This allows one to introduce an effective (photometric) roughness. Unfortunately, for surface topographies with characteristic scale comparable to the particle size the relationship between albedo and surface roughness and their effects on the phase curve is more complex.
(4) Multiple scattering on large-scale topographies with large characteristic angles is important even for surfaces with moderate albedo. Numerous determinations of the roughness parameter of planetary surfaces with the Hapke model appear to be slightly underestimated. This is also important in the analysis of laboratory photometric measurements.
(5) Weak spectral dependences of the roughness parameter in the Hapke model can be explained by a wavelength dependence in the multiple scattering component of the total reflected flux. Comparison of theoretical versus observational data can be re-interpreted with this new understanding.
(6) Prediction of surface roughness from the Hapke model can differ significantly from actual surface roughness for planetary surfaces with large-scale topographies that have several levels of topographic structure.
(7) Particulate media with surface borders described by Gaussian or clumpy topographies with characteristic scale slightly larger than the particle size reveal different photometric behaviors compared to flat particulate surfaces.
(8) The considered surface topography effects do not require radical modifications of Hapke's theoretical model. This model provides a good first approximation for interpretation of planetary surface characteristics. Nevertheless, we hope that our numerical results will stimulate attempts to improve the analytical approach providing benchmarks for verifications of theoretical results.

Acknowledgments

We are grateful to B. Hapke and D. Domingue for many useful remarks. This study was partially supported by INTAS Grant #2000-0792 and by the French National Program of Planetology (PNP/INSU/CNRS). It has also benefited from the support of Paul Sabatier University of Toulouse and Midi-Pyrénées Observatory, with the attribution of visiting positions for Y. Shkuratov and D. Stankevich and the use of computational facilities of the laboratory UMR 5562 "Laboratoire Dynamique Terrestre et Planétaire."

References

Cord, A., Pinet, P., Daydou, Y., Stankevich, D., Shkuratov, Yu., 2002. Planetary regolith surface analogs and mesoscale topography: optimized determination of Hapke parameters using multi-angular spectro-imaging laboratory data. In: Sympos. Solar System Remote Sensing, Pittsburgh, PA. Abstract #4013.

Cord, A.M., Pinet, P.C., Daydou, Y., Chevrel, S., 2003a. Experimental investigation of the potential wavelength dependence of Hapke parameters in the visible and near infrared range. In: Lunar Planet. Sci., vol. 34. LPI Houston. Abstract #1548.

Cord, A.M., Pinet, P.C., Daydou, Y., Chevrel, S., 2003b. Experimental determination of the Hapke shadowing function parameter for planetary regolith surface analogs. In: Lunar Planet. Sci., vol. 34. LPI Houston. Abstract #1349.

Cord, A., Pinet, P., Daydou, Y., Chevrel, S., 2003c. Planetary regolith surface analogs: optimized determination of Hapke parameters using multi-angular spectro-imaging laboratory data. Icarus 165, 414–427.

Grynko, Ye., Shkuratov, Yu., 2003. Scattering matrix for semitransparent particles of different shapes in geometric optics approximation. J. Quant. Spectrosc. Radiat. Transfer 78, 319–340.

Hapke, B., 1981. Bidirectional reflectance spectroscopy. 1. Theory. J. Geophys. Res. 86, 3039–3054.

Hapke, B., 1984. Bidirectional reflectance spectroscopy: 3. Correction for macroscopic roughness. Icarus 59, 41–59.

Hapke, B., 1986. Bidirectional reflectance spectroscopy. 4. The extinction coefficient and the opposition effect. Icarus 67, 264–280.

Hapke, B., 1990. Coherent backscatter and the radar characteristics of outer planet satellites. Icarus 88, 407–417.

Hapke, B., 1993. Theory of Reflectance and Emittance Spectroscopy. Cambridge Univ. Press. p. 450.

Hapke, B., 2002. Bidirectional reflectance spectroscopy. 5. The coherent backscatter opposition effect and anisotropic scattering. Icarus 157, 524–534.

Helfenstein, P., Shepard, M., 1999. Submillimeter-scale topography of the lunar regolith. Icarus 141, 107–131.

Helfenstein, P., Veverka, J., Thomas, P., 1988. Uranus satellites: Hapke parameters from Voyager disk-integrated photometry. Icarus 74, 231–239.

Mishchenko, M., Dlugach, J., Yanovitskij, E., Zakharova, N., 1999. Bidirectional reflectance of flat, optically thick particulate layers: an efficient radiative transfer solution and applications to snow and soil surface. J. Quant. Spectrosc. Radiat. Transfer 63, 409–432.

Muinonen, K., Stankevich, D., Shkuratov, Yu., Kaasalainen, S., Piironen, J., 2001. Shadowing effect in clusters of opaque spherical particles. J. Quant. Spectrosc. Radiat. Transfer 70, 787–810.

Pinet, P., Cord, A., Daydou, Y., Boubault, F., Chevrel, S., Lapeyre, V., 2001. Influence of linear versus non-linear mixture on bidirectional reflectance spectra using a laboratory wide field spectral imaging facility. In: Lunar Planet. Sci., vol. XXXII. LPI Houston. Abstract #1559.

Shepard, M., Campbell, B., 1998. Shadows on a planetary surface and implications for photometric roughness. Icarus 134, 279–291.

Shepard, M., Campbell, B., Bulmer, M., Farr, T., Gaddis, L., Plaut, J., 2001. The roughness of natural terrain: a planetary and remote sensing perspective. J. Geophys. Res. 106, 32,777–32,796.

Shkuratov, Yu.G., 1995. Fractoids and photometry of solid surfaces of celestial bodies. Solar System Res. 29, 421–432.

Shkuratov, Yu.G., 2002. Interpreting photometry of planetary regoliths: progress and problems as seen from Kharkov. In: Sympos. Solar System Remote Sensing, Pittsburgh, PA. Abstract #4011.

Shkuratov, Yu., Grynko, Ye., 2004. Light scattering by semitransparent particles of different shapes and media consisting of these particles in geometric optics approximation: consequences for spectroscopy, photometry, and polarimetry of the planetary regoliths. Icarus, in press.

Shkuratov, Yu., Helfenstein, P., 2001. The opposition effect and the quasi-fractal structure of regolith: theory. Icarus 152, 96–116.

Shkuratov, Yu.G., Stankevich, D.G., 1992. The shadow effect for planetary surfaces with Gaussian mesotopography. Solar System Res. 26, 201–211.

Shkuratov, Yu.G., Starukhina, L.V., Kreslavsky, M.A., Opanasenko, N.V., Stankevich, D.G., Shevchenko, V.G., 1994. Principle of perturbation invariance in photometry of atmosphereless celestial bodies. Icarus 109, 168–190.

Shkuratov, Yu., Kreslavsky, M., Ovcharenko, A., Stankevich, D., Zubko, E., Pieters, C., Arnold, G., 1999. Opposition effect from Clementine data and mechanisms of backscatter. Icarus 141, 132–155.

Shkuratov, Yu., Stankevich, D., Sitko, M., Sprague, A., 2000. Thermal emission indicatrix for rough planetary surfaces at arbitrary heating/observing geometry. In: Sitko, M., Sprague, A. (Eds.), Thermal Emission Spectroscopy and Analysis of Dust, Disk, and Regoliths, vol. 196. ASP, pp. 221–230.

Shkuratov, Yu., Ovcharenko, A., Zubko, E., Miloslavskaya, O., Nelson, R., Smythe, W., Muinonen, K., Piironen, J., Rosenbush, V., Helfenstein, P., 2002. The opposition effect and negative polarization of structurally simulated planetary regoliths. Icarus 159, 396–416.

Shkuratov, Yu., Petrov, D., Videen, G., 2003. Classical photometry of prefractal surfaces. J. Opt. Soc. Amer. A 20, 2081–2092.

Smith, B.G., 1967. Lunar surface roughness: shadowing and thermal emission. J. Geophys. Res. 72 (16), 4059–4067.

Stankevich, D.G., Shkuratov, Yu.G., 1992. Numerical simulation of shadowing on a statistically rough planetary surface. Solar System Res. 26, 580–589.

Stankevich, D., Shkuratov, Yu., 2000. The shadowing effect in regolith-type media: numerical modeling. Solar System Res. 34, 285–294.

Stankevich, D.G., Shkuratov, Yu.G., 2002. Multiple scattering of light in regolith-like media: geometric optics approximation. Solar System Res. 36, 409–416.

Stankevich, D.G., Shkuratov, Yu.G., 2004. Monte Carlo ray-tracing simulation of light scattering in particulate media with optically contrast structure. J. Quant. Spectrosc. Radiat. Transfer, in press.

Stankevich, D., Shkuratov, Yu., Muinonen, K., 1999. Shadow-hiding effect in inhomogeneous and layered particulate media. J. Quant. Spectrosc. Radiat. Transfer 63, 445–458.

Stankevich, D.G., Shkuratov, Yu.G., Muinonen, K.O., Miloslavskaya, O.V., 2000. Simulation of shadings in systems of opaque particles. Opt. Spectrosc. 88, 682–685.

Stankevich, D., Shkuratov, Yu., Pinet, P., Cord, A., 2002. Light scatter by particulate surfaces with different topography. In: Symp. Solar System Remote Sensing, Pittsburgh, PA. Abstract #4010.

Stankevich, D., Shkuratov, Yu., Grynko, Ye., Muinonen, K., 2003. A computer simulation of multiple scattering of light rays in systems of opaque particles. J. Quant. Spectrosc. Radiat. Transfer 76, 1–16.